

The Interactions of High Energy Nucleons with Nuclei. II*

G. BERNARDINI,[†] E. T. BOOTH, AND S. J. LINDENBAUM[‡]
Columbia University, New York, New York

(Received August 1, 1952)

Part I of this paper presented an analysis of the experimentally observed interactions of 300–400 Mev protons and neutrons with the nuclei of *G*-5 emulsion. General evidence for the nucleonic cascade mechanism of interaction was deduced from these results.

Goldberger had previously calculated the interaction of high energy nucleons (~ 90 Mev) with heavy nuclei on the basis of an internal nucleonic cascade generated in a Fermi nucleon gas. However, the experimental test of these calculations by Hadley and York was indecisive.

Calculations basically similar to the Goldberger type were performed for these interactions, employing the Monte Carlo method to treat the rather complicated cascades involved. The theoretical and experimental results are compared in detail and found to be essentially in agreement within error limits. Hence it is concluded that the nucleonic cascade mechanism can satisfactorily explain these interactions.

I. INTRODUCTION

PART I¹ of this paper presented the phenomenological analysis of the nuclear interactions produced in nuclear β -sensitive emulsions by high energy nucleons, i.e., by protons and neutrons of energy 300–400 Mev. Since it was demonstrated that at least 80 percent of the observed interactions were due to collisions of an incident nucleon with the nuclei of the heavy component of the emulsion (AgBr), the observed events should exhibit the general features of the interactions of 300–400 Mev protons and neutrons with the nucleus $A \approx 100$.

The light element interactions could be approximately subtracted from the results by applying the data of Blau and Oliver² obtained using stratified emulsions. However, the differences in light and heavy element events are not sufficiently great that the small percentage of light element events included in the data changes the results appreciably within the statistical and other error limits.

For reasons given in the introduction of Part I,¹ it was felt that these experiments could provide a sensitive test of the nucleon-nucleus collision model previously proposed by Goldberger.³ This paper will report the results of Goldberger-type Monte Carlo calculations for these interactions and compare them with the experiments.

II. THE NUCLEON-NUCLEUS INTERACTION MODEL

The heavy nucleus was represented by the usual Fermi statistical gas theory. In this approximation one considers the ground state of the nucleus as composed of ideal zero temperature noninteracting fermion gases of neutrons and protons bound in a uniform potential

well:

$$\begin{aligned} -|V| & \text{ for } r \leq \text{nuclear radius,} \\ 0 & \text{ for } r > \text{nuclear radius.} \end{aligned}$$

The resulting Fermi-momentum distribution depends upon the effective density of nucleon matter and the temperature.

The simple cubical well solution for the momentum distribution was considered sufficient for these crude calculations and was employed. It can be represented by a sphere of radius equal to the maximum Fermi momentum:

$$P_{\max} = (3h^2/8\pi)^{1/2}(\rho)^{1/2}, \quad (1)$$

where ρ is the effective nucleon density, i.e., number of nucleons per unit volume. The probability that the Fermi momentum of a nucleon will lie in any volume element of the sphere is proportional to the volume. The nuclear radius was calculated from the relationship

$$R = 1.4A^{1/3} \times 10^{-13} \text{ cm.} \quad (2)$$

Since the numbers of neutrons and protons in the nucleus $A=100$ are approximately equal (5:4) and P_{\max} depends only on $\rho^{1/2}$, the value for the average $P_{\max} = 22$ Mev was employed for all nucleons. The average binding energy $-|\alpha|$ per nucleon was assumed to be -9 Mev. Hence the average potential well depth is

$$V = P_{\max} + |\alpha| = 31 \text{ Mev.} \quad (3)$$

The Coulomb barrier for protons was calculated to be about 8 Mev.

The collisions of the incident high energy nucleon ($E \gtrsim 50$ –100 Mev) with the nucleus were treated according to the Serber⁴ point of view. Since the DeBroglie wavelength $\lambda \ll$ nuclear radius, the concept of a definite classical trajectory relative to the nucleus was employed. Because the effective ranges of high energy nucleon-nucleon scattering forces are small in comparison with the mean free path in nuclear matter, it was assumed that the general features of the inter-

* Jointly sponsored by the ONR and AEC.

[†] Now at the University of Illinois, Urbana, Illinois.

[‡] Now at the Brookhaven National Laboratory, Upton, New York.

¹ Bernardini, Booth, and Lindenbaum, *Phys. Rev.* **85**, 826 (1952).

² M. Blau and A. R. Oliver, *Phys. Rev.* **87**, 182 (1952).

³ M. L. Goldberger, *Phys. Rev.* **74**, 1268 (1948).

⁴ R. Serber, *Phys. Rev.* **72**, 1114 (1947).

action are determined by a series of single nucleon-nucleon scattering collisions. Precisely in this approximation the process is represented as a cascade of free nucleon-nucleon scatterings. The influence of the other nucleons is felt only through the potential barrier, the initial Fermi-momentum distribution, and the Pauli exclusion principle which forbids collisions corresponding to final states already filled by other nucleons. Furthermore, the scattering collisions inside nuclear matter are described by asymptotically measured free nucleon-nucleon scattering cross sections.

The Fermi gas nucleus is assumed to remain in the ground state during the development of the internal nucleonic cascade. This is equivalent to stating that the many-body wave functions describing the nucleus are not appreciably affected by the binding forces during the cascade collision time. The cascade proper is considered to continue until either the moving nucleons reach the edge of the nucleus with energy greater than the nuclear (plus Coulomb) barrier and escape, or as a result of a collision the cascade nucleons are degraded in energy below the barrier and are then considered thermally captured. The cascade stage then ends, and the excited nucleus is considered to enter the thermal evaporation stage which will be described by the Weisskopf theory.⁵

This treatment of the problem would clearly become more and more justified as the density of nuclear matter were progressively decreased by an expansion of the nuclear volume. However, as long as the incident nucleon in a collision is characterized by a λ (DeBroglie wavelength) much less than the nuclear diameter, and a mean free path in nuclear matter long compared to the effective scattering ranges, this treatment could perhaps be expected to predict at the very least the gross statistical features of a large number of interactions. This is likely even though each individual calculation was appreciably in error, since the quantum-mechanical departures from this simple semiclassical cascade (which probably corresponds to the mean behavior) would tend to average out when one groups together a large number of interactions. Chew and Wick⁶ have considered the errors involved in these assumptions in their treatment of the impulse approximation and have concluded that, at least for nucleons of energy greater than 50 Mev, multinucleon scattering corrections are not too large. Hence, at least for the faster nucleons, these assumptions may appear reasonable. For those below 50 Mev they certainly become less valid; however, one can hope that the important characteristics of these collisions will still correspond, in general, to the single nucleon-nucleon collision.

In any case the treatment of so complicated an interaction by a simple and crude model cannot possibly

be justified analytically, and one will have to decide its usefulness in the last analysis simply by comparing predictions with experiment.

III. THE GOLDBERGER MODEL CALCULATIONS

A. The Goldberger Work

Goldberger developed the Serber ideas on high energy nucleon-nucleus interactions into a detailed model for calculating these interactions on the basis of the generation of a semiclassical internal nucleonic cascade in a Fermi gas nucleus.

To treat complex cascades of this type and retain all the natural statistical fluctuations he employed the Monte Carlo method.⁷ His original evaluations were performed for the interactions of 90-Mev neutrons with a Pb nucleus. An experimental check of Goldberger's calculations by Hadley and York⁸ was interpreted to be at best only in partial qualitative agreement.

For reasons previously given (see the Introduction of Part I), it was decided that the interaction of 300-400 Mev protons and neutrons, with the Ag-Br nuclei ($A \approx 100$) of β -sensitive emulsion would provide a sensitive test of the model at these higher energies, where it would be expected to be intrinsically more reliable. Some general evidence for the internal nucleonic cascade was deduced from the experimental results described in Part I.¹ In this paper detailed calculations of the Goldberger type for these interactions will be described and the results compared with the experimental data.

B. The Monte Carlo Method

The Monte Carlo Method⁷ is a generally valid procedure for treating an ordered sequence of processes ($A, B, C \dots$) each of which is characterized by its own statistical distribution. One divides each statistical distribution into equally probable intervals, and then starting with a random choice for A chooses in sequence at random equally probable events for B , then for C , etc., until one finally arrives at the end state. It is obvious that for sufficiently fine intervals what one does is to merely naturally reproduce the process, and hence the inherent statistical fluctuations in the final state distribution curves should be the same for N Monte Carlo calculations as one obtains for results based on N experimentally observed events. Of course, this assumes that the statistical distribution curves put into the calculations are correct and completely describe what happens. The manner of application of the method to the present problem will be made clear by a description of the procedure.

⁵ V. Weisskopf, Phys. Rev. **52**, 295 (1937).

⁶ G. Chew and G. C. Wick, Phys. Rev. **85**, 636 (1952).

⁷ S. Ulam and J. VonNeumann, Bull. Am. Math. Soc. **53**, 1120 (1947).

⁸ J. Hadley and H. York, Phys. Rev. **80**, 345 (1950).

C. The Mean Free Path in Nuclear Matter

The cross section for $p-p$ scattering has been experimentally investigated from 18 Mev to 340 Mev.⁹⁻¹¹ It was found to be essentially isotropic in the c.m. system at all energies, to be essentially constant in magnitude from 340-120 Mev, to increase more slowly than a $1/\text{energy}$ law between 120 and 31 Mev, and to follow a $1/\text{energy}$ law from 31 Mev to 18 Mev. The circled points of Fig. 1 represents the experimental points, and the solid curve down through them represents the variation with energy assumed for these calculations.

The $n-p$ cross section has been investigated from 40-270 Mev.¹²⁻¹⁴ It was found to be anisotropic in the center-of-mass system, and characterized by a rather flat valley around 90° with symmetrical sharp peaks in the forward and backward directions. The effect of these peaks is sharply reduced inside nuclear matter by the Pauli exclusion principle, which discourages small momentum transfer collisions. Hence it was felt that a simplification could be introduced by replacing the $n-p$ cross section by an equivalent isotropic cross section chosen so as to yield the same average energy transfer as the actual anisotropic cross section. It was found in all cases that the equivalent isotropic cross section differed only slightly in magnitude from the average height of the valley in the region of the $n-p$ scattering curve around 90° . This demonstrates that the energy transfer characteristics are mostly determined by this region and are not much affected by the forward and backward peaks.

The total cross section of the equivalent isotropic curve was reduced by at most 30 percent from the original. The actual reduction after taking into account the Pauli exclusion principle would be much smaller. The equivalent isotropic $n-p$ cross section as a function of energy is given by the dashed curve in Fig. 1. The circled points were fitted by a smooth curve of the form $1/E^\alpha$, where $0 \leq \alpha \leq 1$. The extrapolation of the $p-p$ curve to higher energies (~ 400 Mev) is fairly reliable since the curve is constant over the large region 120-340 Mev, and it is unlikely that it would change suddenly. The $n-p$ extrapolation is not so reliable, but it is a reasonable guess.

The mean of the $p-p$ and $n-p$ curves is represented by the dash-dot curve of Fig. 1. At the higher energies the mean is quite close to the individual cross sections, but at the lower energies the separation of the $n-p$ and $p-p$ curves becomes appreciable. It is generally assumed that nuclear forces are charge independent; therefore, one should expect that $\sigma_{n-n} \approx \sigma_{p-p}$. Inelastic

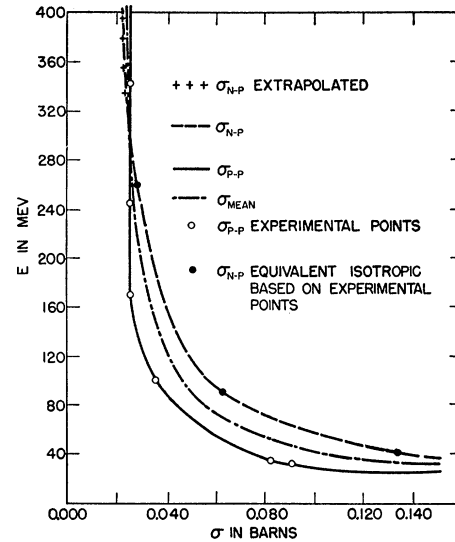


FIG. 1. The nucleon-nucleon scattering cross sections as a function of energy.

cross section measurements with high energy neutrons^{14,15} generally agree with this assumption. Furthermore, the similarity of the neutron stars to the proton stars, as reported in Part I, is further evidence for this assumption.

The calculations are greatly simplified if one treats a nucleonic cascade of nucleons without regard to their charge identity. Since the shape of the differential cross sections is considered the same (i.e., isotropic), the number of neutrons and protons is roughly equal, and the mean total cross-section curve does not differ too drastically from the individual curves, one can approximately replace the neutrons and protons by a single type of nucleon whose cross section is equal to the mean cross section and whose density is equal to the mean nucleon density. This approximation will be expected to give reasonable results for the characteristics of all nucleons, that is, neutrons and protons taken together, but will lead to uncertainties in the ratio of protons to neutrons. This point will be considered later, and it will be shown that it is probable that the emitted nucleons are roughly half neutrons and half protons.

The mean cross section given in Fig. 1 as a function of the moving nucleon energy must of course be averaged over the Fermi sphere. The probability W_i of a collision with a nucleon in a volume element of the Fermi sphere dV_i is

$$W_i = \text{const} \sigma(P_{r_i}) P_{r_i} dV_i, \quad (4)$$

where P_{r_i} is the momentum of the incident nucleon relative to the target nucleon.

With the exception of the low energy region the mean cross section varies in a manner not too different from

⁹ Chamberlain, Segrè, and Wiegand, Phys. Rev. **81**, 661 (1951)

¹⁰ B. Cork, Phys. Rev. **80**, 321 (1950).

¹¹ W. Birge, Phys. Rev. **80**, 490 (1950).

¹² Hadley, Kelly, Leith, Segrè, Wiegand, and York, Phys. Rev. **75**, 351 (1950).

¹³ Kelly, Leith, Segrè, and Wiegand, Phys. Rev. **79**, 96 (1950).

¹⁴ Cook, McMillan, Peterson, and Sewell, Phys. Rev. **75**, 7 (1950).

¹⁵ Fox, Leith, Wouters, and MacKenzie, Phys. Rev. **80**, 23 (1950).

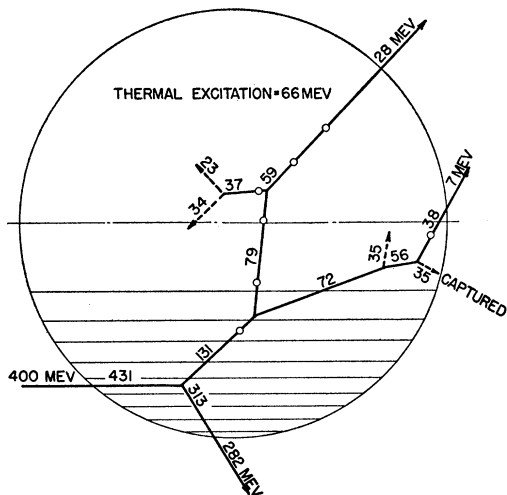


FIG. 2. A work diagram used in the two-dimensional calculations, illustrating the actual development of an interaction. The circle represents the cross section of a nucleus of mass number 100. Its radius is taken to be $R = 1.40A^{1/3} \times 10^{-13}$ cm.

a const/P_{r_i} law. Hence,

$$\sigma(P_{r_i})P_{r_i}dV_i = \text{const}dV_i = W_i, \quad (5)$$

and, therefore, the average cross section over the Fermi sphere is the same as the mean cross section for the incident energy. In the low energy region the mean cross section varies like a $1/\text{energy}$ law, and it can be easily shown that in this case also the average cross section over the Fermi sphere is the same as the mean cross section for the incident energy. Hence, the mean free path is a function of energy,

$$\lambda(E) = 1/\rho\bar{\sigma}(E), \quad (6)$$

where E is the energy of the moving nucleon inside the nucleus, ρ is the density of the nucleons, and $\bar{\sigma}(E)$ is the mean cross section as a function of energy given in Fig. 1.

The path length distribution inside the nucleus is obviously given by the following distribution law:

$$q = e^{-x/\lambda(E)}, \quad (7)$$

where q is the probability of a collision not having occurred in a distance x inside the nucleus. The distribution of path lengths is taken into account by dividing q into 1000 equally probable intervals and picking one at random. To each interval, of course, there corresponds a particular value of $x/\lambda(E)$ given by Eq. (6). Evaluating $\lambda(E)$ from Eq. (6) yields the particular path length.

D. The Two-Dimensional Geometry

One is concerned here with the interaction of a parallel beam of high energy nucleons with a spherical nucleus of uniform density. The momentum distribution of the nucleons inside the nucleus is spherically symmetric and characterized by a Fermi sphere. The

experimentally determined nucleon-nucleon scattering cross sections all possess polar symmetry around the line of mutual approach in the center-of-mass system. Therefore, it is obvious that there must be a polar symmetry around the incident beam direction for all final distribution curves. This polar symmetry around the incident beam direction suggests that the problem might be considerably simplified by an appropriate two-dimensional treatment. This is necessary, as a three-dimensional treatment would be prohibitively lengthy. Let us replace the three-dimensional spherical nucleus with a two-dimensional great circle, of which a diameter is chosen to be along the incident beam direction. A three-dimensional factor which we must incorporate in our two-dimensional treatment is that segments of this circle formed by a series of chords parallel to the beam direction must be weighted proportionately according to the ring area they present normal to the incident beam. The division of half the circle of nuclear radius into ten such weighted segments is shown in Fig. 2. Only half a circle was used for convenience since the final distributions are symmetrical around the beam direction. By considering equal numbers of incoming nucleons incident upon each of the ten segments, one weights the initial geometry according to the true three-dimensional case.

The three-dimensional Fermi sphere was transformed into a two-dimensional circle of the same radius, such that the two-dimensional polar angle corresponds to the original three-dimensional polar angle relative to the incident nucleon direction. However, the two-dimensional polar angle now has positive and negative values in order to take into account the fact that the resultant vector momentum can be directed toward the center of the two-dimensional nucleus or away from it. The resultant two-dimensional area elements are weighted according to the three-dimensional volume elements corresponding to their rotation about the incident beam direction.

The division of the three-dimensional Fermi sphere into 1000 equal volume elements is given in terms of this correspondingly weighted two-dimensional repre-

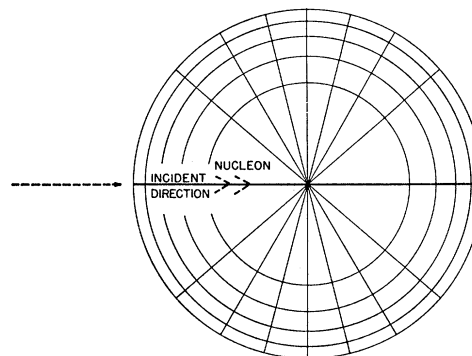


FIG. 3. The Fermi momentum sphere. The Fermi sphere used in the calculations contained 1000 volume intervals; the above sphere contains only 80 for illustrative purposes.

sensation in Fig. 3. When a collision takes place, the relative probability for the target nucleon to lie in the volume element dV_i of the Fermi momentum sphere is seen from Eq. (5) to be proportional to dV_i , for all but the low energy region. Therefore, equal volume elements represent equal collision probabilities, and hence the appropriate choice of a collision partner for the moving nucleon is a random choice of one of the equal 1000 volume elements represented by Fig. 3. The low energy region would require a different weighting of the Fermi sphere; but this only affects the tail end of the nucleonic cascade, and it is felt that the results will not be affected much by the use of the same Fermi sphere weighting throughout.

This procedure insures that the kinetics of the scatterings such as energy transfer and relative angle between the two nucleons involved in a collision will be preserved in these two-dimensional calculations.

E. The Scattering Calculation

From the directions and momenta of the incident nucleon and the target nucleon, one calculates the kinetic relations in the center-of-mass system before the collision. All differential cross sections are assumed to be isotropic; hence, the appropriate division of the scattering angle θ into equal probability intervals is according to equal cosine θ intervals.

The choice of a scattering angle interval at random then enables one to calculate completely the angles and energies of the scattered nucleons. Relativistic calculations were used for an incident energy > 150 Mev. Non-relativistic calculations were used for energies below 150 Mev. If the final energy of either scattered nucleon was less than 22 Mev (top of the Fermi sphere), the collision was forbidden by the Pauli exclusion principle and was assumed not to have taken place. The use of the mean free path for free nucleons, the subsequent calculation of the scattering collisions, and then finally the application of the Pauli principle is merely a matter of calculatory convenience. It can be shown that the appropriate reduction of the scattering cross section to only those parts which lead to allowed collisions yields the same results as the above procedure.

F. The Barrier

In Sec. II it was shown that the average nuclear well depth is 30.6 Mev and the Coulomb barrier is 8 Mev for protons. Since we are treating average nucleons in this calculation, the average Coulomb barrier is about 4 Mev. Therefore, the total average nuclear barrier is about 35 Mev. Hence, it is assumed that if, after any collision, a nucleon has an energy of less than 35 Mev, it is thermally captured. A nucleon which reaches the edge of the nucleus must for consistency lose a kinetic energy equal to the well depth (31 Mev) upon escaping. Reflection and refraction by the barrier are neglected.

G. The Working Procedure

Figures 2 and 4 are replicas of actual work diagrams. Equal numbers of 400-Mev nucleons were considered incident upon each of the ten ring area weighted segments shown in the figures. Upon entering the nucleus the 400-Mev nucleons gained the 31-Mev nuclear potential. The mean free path for 431-Mev nucleons was calculated according to Eq. (6), Sec. II-C. A random number table was used for all random choices. A three-place random number was chosen to select one of the 1000 equally probable intervals for $x/\lambda(E)$, given by Eq. (7). Having already calculated $\lambda(E)$, x was obtained, and the incoming nucleon trajectory was extended a distance x beyond its entrance point. If x fell outside the nucleus, this was considered to represent the phenomenon of nuclear transparency. If x fell inside, a collision was assumed to attempt to take place at x .

A second random number was chosen to select one of 1000 equally probable Fermi momentum intervals (shown in Fig. 3). The Fermi momentum and direction together with the incoming nucleon momentum and direction were used to calculate relativistically the kinetic characteristics in the center-of-mass system before the collision. A third random number was chosen to select a scattering angle interval. The scattering angle was introduced, and the calculation was completed relativistically to yield the final angles and energies of the scattered nucleons. These were plotted on the diagram as shown in Figs. 2 and 4. If the final energies of either nucleon fell below 22 Mev (the top of the Fermi sphere), the collision was assumed not to have occurred and the incident nucleon was given a

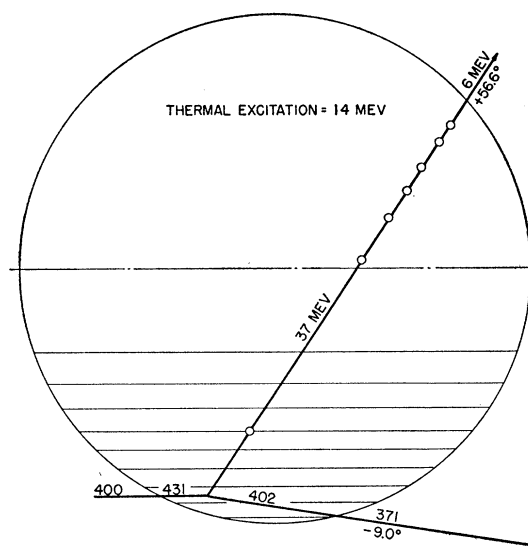


Fig. 4. Another work diagram used in the two-dimensional calculations, illustrating the actual development of an interaction. The circle represents the cross section of a nucleus of mass number 100. Its radius is taken to be $R = 1.40A^{1/3} \times 10^{-13}$ cm.

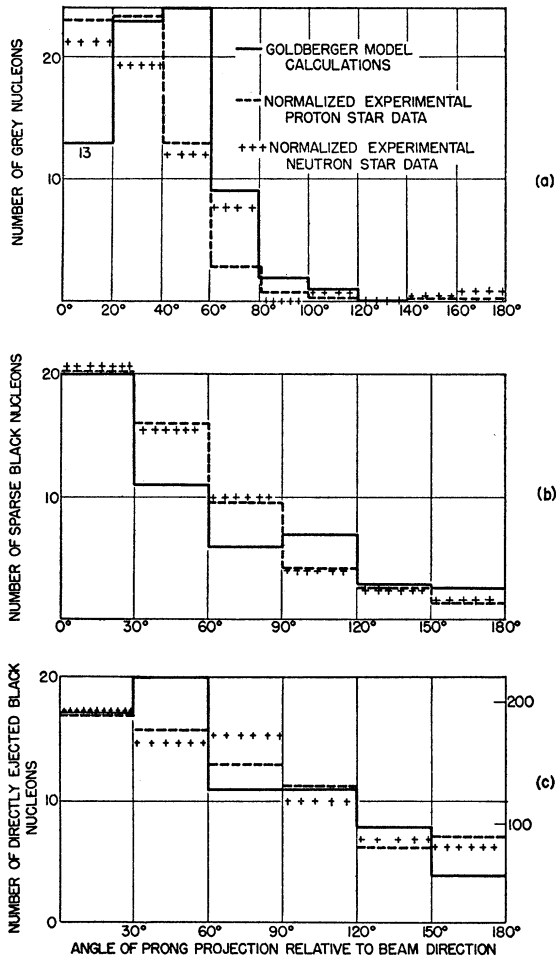


FIG. 5. A comparison of the calculated and experimental: (a) gray (>100 Mev) nucleon angular distribution; (b) sparse black (30–100 Mev) nucleon angular distribution; (c) black (≤ 30 Mev) nucleon angular distribution.

new path length (chosen at random) along the original direction.

In Figs. 2 and 4 the first collision occurred. Each of the two moving nucleons resulting from the first collision was then given a path length (at random) along their plotted directions. The appropriate $\lambda(E)$ for each energy was used.

The previous procedure for the incident nucleon was followed for all products of the cascade until either they reached the edge of the nucleus and escaped with a loss of 31 Mev, or their energy fell below the nuclear barrier (35 Mev) and they were considered captured (as illustrated). The circles along the trajectories indicate positions where collisions attempted to take place but were forbidden by the Pauli principle.

As previously discussed, due to symmetry, only the magnitude of the angles of the emergent prongs relative to the incident beam direction has significance. The sign is meaningless.

H. The Thermal Excitation

One can write the conservation of energy equation for these interactions as

$$400 = \sum_{n=1}^N E_n + |\alpha|(N-1) + U, \quad (8)$$

where N is the number of emergent nucleons, $|\alpha|$ is the nucleon binding energy, and U is the thermal excitation. The 400 on the left side represents the incident energy. The term $\sum E_n$ on the right side represents the sum of the kinetic energies of the N emergent nucleons, and $|\alpha|(N-1)$ represents the binding energy of the emergent nucleons. The -1 is due to the fact that the incoming nucleon is not bound. Hence, it is clear that U must represent the thermal excitation. Solving for U , one has

$$U = 400 - \sum_{n=1}^N E_n - |\alpha|(N-1). \quad (9)$$

The thermal excitation so defined represents the sum of two effects. These are the direct contribution of thermally captured nucleons, and the excitation energy represented by the holes left in the Fermi distribution by the directly ejected target nucleons. These two effects are roughly comparable in magnitude.

I. Interpretation of Results

The two-dimensional treatment used in the calculations suggests that probably a reasonable comparison of the calculated angular distributions and the experimental projected angular distributions can be made. Of course, the two angles do not correspond in any exact manner, but they both have similar two-dimensional characteristics and it is reasonable to expect that the important features of the distributions would be common to both.

The calculations performed give the numbers of neutrons and protons emitted lumped together as a total number of nucleons. The estimation of the ratio of emitted protons to neutrons is a rather difficult one to make. This ratio depends in a complex way upon the charge of the incident nucleon, the relative values of $p-p$, $n-n$, and $n-p$ scattering cross sections, the relative numbers of neutrons and protons, and the number of collisions inside the nucleus. The average ratio of protons to neutrons is about 5:4 and could be roughly considered equal to 1. The assumption of charge independence of nuclear forces is made, and therefore $\sigma_{n-n} \approx \sigma_{p-p}$. Figure 1 shows that over the high energy regions $\sigma_{n-p} \approx \sigma_{p-p}$. Hence, $\sigma_{n-p} \approx \sigma_{p-p} \approx \sigma_{n-n}$.

One would expect the ratio of fast protons to neutrons to be statistically weighted in favor of the incoming charge after the first collision. A very rough estimate of this factor would be about 3:1, since only half of the $n-p$ cross section (the exchange half) yields fast neutrons, while most of the $p-p$ cross section and

the nonexchange half of the $n-p$ yield fast protons. After a few collisions (estimated 2-3), the ratio would begin to approach 1, since this statistical factor is very rapidly reduced by the inherent symmetry of our assumed cross sections. Furthermore, the excess number of neutrons and the faster rise of the $n-p$ cross section with decreasing energy than the $p-p$ would also tend to reduce this ratio.

Since the average number of nucleon-nucleon collisions found per interaction in the calculations is about 4.5, it is reasonable to assume that approximately equal numbers of protons and neutrons are ejected in these interactions.

The similarity of the neutron and proton induced interactions reported in Part I provides direct experimental evidence for the validity of this assumption.

IV. COMPARISON OF GOLDBERGER CALCULATIONS WITH EXPERIMENTAL RESULTS

A. Introduction and Terminology

The results described in this chapter are based on 90 incident 400-Mev nucleons, of which 60 resulted in inelastic events and 30 went through the nucleus without interacting. Within statistics this division agrees with the expected calculated reduction of the geometric cross section by about 35 percent due to nuclear transparency.

In order to compare the results with the experimental proton and neutron star data, the same terminology was used in classifying the emitted nucleons as gray, sparse black, or black corresponding to kinetic energy greater than 100 Mev, between 100 and 30 Mev, and less than 30 Mev, respectively. To correspond to the experimental terminology, "prong" is used as a synonym for "emitted nucleon."

B. Angular Distributions

The comparison is made directly with projected experimental angles as discussed under "Interpretation of Results" in Sec. III. Figure 5(a) is a comparison of the calculated gray prong angular distribution with the experimental proton and neutron star gray prong angular distribution. Figure 5(b) is a comparison of the calculated sparse black prong angular distribution with the experimental proton star sparse black prong angular distribution. The agreement in both cases is reasonable within statistical limits. However, there seems to be a tendency for the experimental gray curve to be somewhat lower, and the experimental sparse black curve to be somewhat higher, in the forward half plane. This could represent a real experimental technique effect due to the erroneous inclusion of some border gray prongs in the sparse black region.

Figure 5(c) presents the directly ejected black prong angular distribution. An exact comparison with the experimental results was not possible in this case, since the evaporation and light element star components are

included in the experimental curve. However, if one normalizes the experimental curve to the same total number [this was done in Fig. 5(c)], one can see a general agreement in the shapes of the curves. The additional isotropic component in the experimental curve is what one would expect as due to the evaporation and light element star components.

C. Mean Prong Numbers

The experimental results for neutron and proton induced interactions have already been compared in Part I¹ and shown to be in reasonable agreement within the energy differences involved and the added difficulties in detecting small neutron events. Since the proton interactions are the ones on which the actual calculations were based and are also the most complete, the comparison will be made with their results.

Table I, line (a), lists the mean numbers per interaction of directly ejected sparse black and gray nucleons. In Sec. III of Part I, it was concluded that a reasonable assumption for the fraction of emitted nucleons which are protons is $\frac{1}{2}$. Using this factor, line (b) of Table I is an estimate of the mean number of directly ejected sparse black and gray protons per event. Line (c) is the experimentally determined mean number per proton star.

The agreement is reasonable for the statistical limits given. However, there seems to be a systematic tendency for calculated values to be slightly higher than experimental values. This is what one expects due to the loss of zero prong stars in the area scanning which are rich in fast prongs. A correction for this could have been applied and would have led to an even closer agreement. However, this was not considered worth while, since one is already within statistical and other error limits.

This systematic experimental underestimation of fast prongs will of course operate in all comparisons.

The black prongs require special considerations, as one must add the estimated evaporation contribution to the mean number of directly ejected protons. Furthermore, the conclusions reached about the black prongs will be expected to be less reliable than those pertaining to the faster nucleons, for several reasons. First, the general validity of the model becomes questionable at these low energies, since the range of free scattering forces becomes larger than the nucleon radius, and hence, the effects of multiple interactions

TABLE I. Comparison of experimental and calculated mean numbers of gray and sparse black protons.

Line	Sparse black	Grey
(a) Mean No. of directly ejected nucleons	0.83 ± 0.16	1.2 ± 0.22
(b) Estimated mean No. of protons	0.42 ± 0.1	0.6 ± 0.12
(c) Experimental mean No. of protons	0.35 ± 0.04	0.42 ± 0.04

TABLE II. Comparison of experimental and calculated mean numbers of black prongs.

Line (a)	Mean No. of directly ejected black nucleons	1.15 ± 0.22
Line (b)	Estimated mean No. of directly ejected protons	0.58 ± 0.12
Line (c)	Estimated mean No. of evaporation prongs	1.5 ± 0.2
Line (d)	Estimated Mean No. of visible black prongs	2.1 ± 0.4
Line (e)	Experimental mean corrected value	2.5 ± 0.2

with more than one nucleon can be important. Reflection and refraction effects at the nuclear surface, which are neglected, can also be important and change the results appreciably. It is also doubtful whether a moving nucleon of kinetic energy close to the well depth can be considered as interacting with a free particle gas of nucleons in the potential well. Furthermore, in treating the evaporation contribution to the black prongs, one is confronted with the lack of knowledge of the relation between nuclear temperature and entropy, and must rely on empirical results for the relation between excitation and number of evaporation prongs. These are not too reliable, due to inherent mixing of knock-ons and evaporation prongs; and also the effects of the Coulomb barrier at low excitations cannot be estimated well due to lack of knowledge of the temperature. In addition, it is very doubtful that temperature equilibrium can even be established in an evaporating Fermi nucleus, due to the relatively weak coupling for the statistical sharing of energy.

Nevertheless, it can be hoped that these difficulties will not be too serious, and it is worth while to attempt to take the calculations seriously even for the black prongs and see what results one gets. As we shall see shortly, even the black-prong-predicted results seem to agree with the experimental determinations.

The mean number of directly ejected black nucleons is given in line (a) of Table II. The estimated mean number of black protons is given in line (b). The calculated average thermal excitation for all interactions is 50 Mev. To estimate the number of black prongs corresponding to this average excitation, we shall use the value of 35-Mev excitation per black prong experimentally determined by Bernardini *et al.*¹⁶ from similar cosmic-ray stars. Undoubtedly there were appreciable numbers of knock-ons in the spectrum used. Also, we are extrapolating to lower excitation energies perhaps without justification. However, it is the best estimate that can be made at the present time. A thermal excitation of 50 Mev would then be expected to yield a mean evaporation contribution of 1.5 black prongs per interaction. One should also include a statistical error due to the limited number of interactions. This expected evaporation mean prong number is given in

¹⁶ Bernardini, Cortini, and Manfredini, Phys. Rev. **79**, 952 (1950).

line (c) of Table II. The sum of lines (b) and (c) is given in line (d) and is the theoretical prediction for the mean observed prong number. The experimental mean value is given in line (e), and is in reasonable agreement.

From Table II, lines (b) and (d), one can calculate the percentage of visible black prongs which are knock-ons. The result is that 28 percent \pm 7 percent of the visible black prongs are expected to be knock-ons. In Part I,¹ the experimental result was that at least 25 percent of the black prongs are knock-ons. Hence, the results seem to agree. However, the experimental value was determined by assuming that the isotropic component of the black prong distribution curve was entirely due to evaporation and did not contain any isotropic knock-on component. An inspection of Fig. 5(c) reveals that there is an isotropic component in the knock-ons. The value of this isotropic component is difficult to estimate because the statistics are very limited; and secondly, the shape of the directly ejected black prong distribution curve cannot be considered too reliable, since refraction effects, etc., at the edge of the nucleus could change the distribution considerably.

Considering the ordinate in the extreme backward direction of Fig. 5(c) as the average knock-on isotropic ordinate, the predicted percentage of forwardly projected knock-ons is about 20 ± 5 percent, and is still in reasonable agreement with the experimental estimate.

D. Distribution of Interactions with Gray or Sparse Black Protons

The distribution of stars as a function of the number of fast (gray or sparse black) prongs provides a sensitive test of the nucleonic cascade mechanism. It has already been demonstrated from their angular distributions (see Part I¹) that they are definitely knock-ons, and hence their frequency distribution should be expected to reflect the nature of the type of internal nucleon cascade involved (i.e., single nucleon-nucleon scatterings or scatterings involving several nucleons).

The angular distributions, and mean prongs number have already been found to agree with the single nu-

TABLE III(a). Comparison of experimental and calculated distribution of gray proton interactions. (b) Comparison of experimental and calculated distribution of fast proton interactions.

(a)		
No. of gray protons	% of interactions calculated	% of interactions experimental result
0	46 ± 11	57 ± 4
1	48 ± 11	40 ± 4
2	7 ± 4	2.5 ± 1
(b)		
No. of fast protons	% of interactions calculated	% of interactions experimental result
0	30 ± 7	35 ± 3
1	48 ± 8	54 ± 4
2	21 ± 7	9 ± 2
3	3 ± 1.5	1.7 ± 0.7

cleon-nucleon scattering hypothesis. Tables III(a) and (b) list the experimentally determined percentages of events with various numbers of outgoing gray protons, and fast (gray plus sparse black) protons. As previously discussed, the appropriate assumption for estimating the numbers of emitted protons is that of equally probable proton or neutron emission. Using this relation, the estimated distributions of gray proton events and fast (gray plus sparse black) proton events are also given in Tables III(a) and (b) and are in reasonable agreement with the experimental results.

E. The Energy Spectrum

The energy spectrum of the directly ejected nucleons is given in Fig. 6(a). The mean number of gray, sparse black, and black nucleons has been shown to be in agreement with the experimental results in Sec. C. The characteristics of G-5 plates allowed only an energy determination for the gray prongs which was reported in Part I.¹ The experimentally determined gray prong spectrum is compared to the calculated one in Fig. 6(b) and is in reasonable agreement. It should be noted that the large peak of the knock-on nucleon spectrum, which occurs in the black prong region (0-30 Mev), is suspiciously similar in appearance to the type

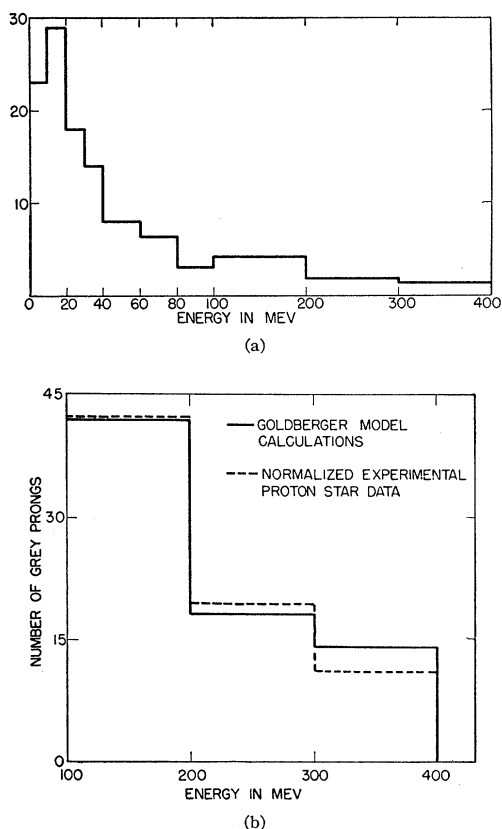


FIG. 6(a). The energy spectrum of the knock-on nucleons directly ejected. (b) A comparison of the calculated and experimental gray (>100 Mev) nucleon spectrum.

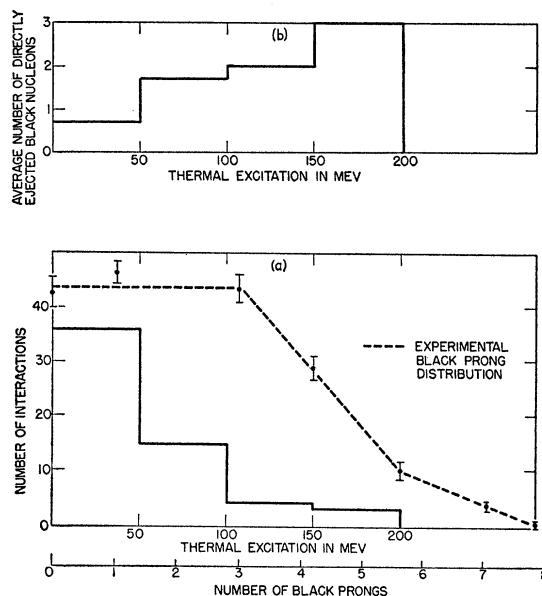


FIG. 7(a). The distribution of interactions as a function of thermal excitation and the experimental black prong distribution curve are given. The relationship of 35 Mev per black prong (as explained in text) was used to convert thermal excitation to number of black prongs. (b) The average number of directly ejected black nucleons as a function of thermal excitation.

of spectrum interpreted in cosmic-ray stars by Le Couteur¹⁷ and others as an evaporation spectrum.

The percentage of the black prongs which are calculated to be knock-ons is about 30 percent. Therefore, it is clear that the knock-on black prongs are approximately comparable in number and are probably similar in energy characteristics to the evaporation prongs.

It is possible in our interactions to separate most of the knock-ons from the evaporation prongs by the difference in angular distribution. However, an inspection of Fig. 5(c) shows that the knock-on black prong angular distribution is approaching isotropic except for the extreme backward direction. When one selects large stars, such as Le Couteur,¹⁷ who treated 7-14 prong stars, it is expected, on this model at least, that the black prong angular curve will become practically isotropic. This is so because large stars mean large nucleonic cascades, in which the preference for the incoming direction is lost by many collisions. For instance, in the present calculations the largest events corresponded to 16 nuclear collisions. In the case of large stars there is probably no experimental way of separating the knock-ons from the evaporation protons.

F. The Thermal Excitation Distribution

Figure 7(a) represents the distribution of events *versus* thermal excitation in Mev. One should notice that the average thermal excitation of 50 Mev is only a small fraction of the incident 400 Mev. The maximum excitation was found to be only about 200 Mev. This is

¹⁷ K. J. Le Couteur, Proc. Phys. Soc. (London) A63, 259 (1950).

a result of the high transparency of the nucleus to the incoming nucleon and its collision products.

One expects, on the basis of the Weisskopf thermodynamical model, that the average number of black prongs emitted is roughly linearly proportional to the thermal excitation (see LeCouteur¹⁷). Therefore, one would expect the horizontal axis to be roughly proportional to the emitted black prong number. (Using Bernardini's¹⁶ value of 35 Mev per black prong, the cutoff of the thermal excitation curve at 200 Mev would correspond to about 6 black prongs.) The shape of the prong distribution curve due to evaporation would be expected to be similar to the thermal excitation distribution curve of Fig. 7(a) if the horizontal axis were relabeled in terms of black prongs, with each 35 Mev of excitation corresponding to an additional black prong. This would disagree with the shape of the experimental black prong distribution [also plotted in Fig. 7(a)], which is seen to be flatter in the region of 1 to 4 black prongs (corresponds to 35–160 Mev excitation) and to decrease more gradually thereafter.

Consider Fig. 7(b) plotted above the thermal excitation distribution. Figure 7(b) represents the average number of directly ejected black nucleons as a function of thermal excitation. On the average, half of these will be protons, and this increasing number of directly ejected protons as a function of thermal excitation (or equivalently mean prong number) is just what is needed to flatten the black prong distribution curve in the region of 1–4 prongs and to extend its tail appropriately. In particular, the stars corresponding to 200-Mev excitation have an expected mean prong number of about 6. The average number of ejected protons is 1.5 in this region. Therefore, the effective cutoff (neglecting fluctuations) would be expected at about 7.5 black prongs, which is reasonable compared with the experimental results. The addition of these two effects (evaporation plus knock-on), together with a reasonable allowance for the fluctuations, seems to present a mechanism which in a very crude way would reproduce the essential features of the black-prong distribution curve.

V. CONCLUSIONS

A detailed comparison of all the experimentally measured characteristics of the interactions of 300–400 Mev protons and neutrons and the Goldberger model calculations has been made. The results were all in reasonable agreement within the error limits, and hence it appears safe to assume at the very least that the internal nucleonic cascade mechanism is useful as a calculatory tool for high energy interactions ~ 400 Mev.

Furthermore, the very nature of the results very strongly implies the necessity of this mechanism for their explanation. Consider the gray (> 100 Mev) and sparse black (30–100 Mev) protons. It has already been experimentally demonstrated by their angular dis-

tributions that they are definitely almost exclusively knock-ons. Hence, the only question that remains is whether the cascade in which they originated essentially consists of single nucleon-nucleon scatterings or some sort of multiple nucleon scatterings.

Our results are that the angular distributions, mean numbers, energy spectrum, and the frequency of interactions as a function of the numbers of these fast knock-ons are all in agreement with the single nucleon-nucleon cascade hypothesis. Since these calculated cascades are rather large (average number of collisions = 4.5, maximum number = 16) one should definitely expect any multiple nucleon type of internal cascade to have entirely different characteristics. Furthermore, (see arguments given in Part I¹ under Discussion) the abundance of black knock-on prongs (at least 25–40 percent), the steady transfer of energy from the fast nucleons to the black nucleons as star size increases, and the similarity of the properties of proton and neutron induced interactions all strongly imply the nucleonic cascade mechanism.

In order to determine whether the model breaks down at lower energies (~ 100 Mev) as perhaps implied by the Hadley and York⁸ results, a similar investigation is being carried out for the interactions of 150-Mev protons with the emulsion nuclei. Preliminary results have indicated that it is quite reliable even at these lower energies. At higher energies (in the Bev range) it is obvious that inelastic processes such as meson production and their subsequent interaction with the nucleus will drastically alter this simple mechanism. However, it is possible that the inclusion of these processes in the calculations (provided they are known and are sufficiently simple) will still make this type of approach useful.

One should point out that since their discovery in cosmic ray by Blau and Wambacher,¹⁸ the nuclear stars have been submitted to a very large number of experimental and theoretical analyses. The general tendency was to consider them mostly as an evaporation process following a very high internal excitation of the evaporating nucleus. This tendency was emphasized by the early type of plates used like Ilford C-2 which were insensitive to the more energetic prongs. The results of the analysis presented in this paper imply that the residual nuclear excitation responsible for evaporation is quite low and that the essential process which determines the characteristics of the stars is the internal nucleonic cascade generated. The evaporation contribution is only more or less a by-product of the cascades.

The authors are indebted to Mr. Leon Landovitz and Mr. Jack Leitner for their excellent work in performing the Monte Carlo computations.

¹⁸ M. Blau and H. Wambacher, *Sitzber. Akad. Wiss. Wien, Math.-naturw. Kl. Abt. IIa*, **146**, 259, 469, 623 (1937).